Available online at www.sciencedirect.com

ScienceDirect

Physics Procedia 56 (2014) 1343 – 1352

Physics Procedia

8th International Conference on Photonic Technologies LANE 2014

Residual stress formation relating to peak temperature- and austenite grain size-based phase transformation of S355 steel

Fabian Klaproth[a,]*, Frank Vollertsen[b]

[a] BIAS - Bremer Institut für angewandte Strahltechnik, Klagenfurter Straße 2, 28359 Bremen, Germany
[b] BIAS - Bremer Institut für angewandte Strahltechnik and University of Bremen, Klagenfurter Straße 2, 28359 Bremen, Germany

Abstract

Nowadays thermal forming processes of steel are state of the art in industrial applications. Nevertheless, the influences of thermal induced phase-transformation on residual stresses and strength have not been fully observed.
Times needed for transformation are affected by the initial austenite grain size, while the prevailing peak temperature influences austenite grain growth. Higher temperatures lead to larger austenite grains, leading to increased times for transformation.
In order to get an embraced understanding of such effects numerical simulations of phase-transformations are mandatory. In this paper simulations of thermal forming processes, using S355 steel, are presented. Different continuous-cooling-transformation-diagrams (cct-diagrams) of specific austenite grain sizes for temperatures between transformation point AC3 and melting temperature are implemented in the model. It is shown that resulting magnitudes of residual stresses vary between 248 N/mm² and 550 N/mm². Finally an approach for the impact on relevant peak temperatures in the heat affected zone is outlined.

Peer-review under responsibility of the Bayerisches Laserzentrum GmbH

Keywords: simulation; phase transformation; residual stress; S355 steel; thermal forming

1. Introduction and motivation

Thermal bending is a technique for flexible forming, Jeswiet et al. (2008) pointed out its significance and development in forming processes. The worth for contemporary applications and high strength steels is shown by Neugebauer et al. (2009) who use the local laser heat treatment to improve formability. Vollertsen (1996) gives a

* Corresponding author. Tel.: +49-421-281-58109 ; fax: +49-421-218-58063 .
E-mail address: klaproth@bias.de

Peer-review under responsibility of the Bayerisches Laserzentrum GmbH
doi:10.1016/j.phpro.2014.08.061

deep insight into thermal forming and its basic mechanisms. Vollertsen (1993) also describes an analytical way for modelling of laser bending for an application under simplified conditions. This approach is not transferable to complex three-dimensional components. Because of that nowadays numerical simulations of thermal forming processes are well established and widely used, so for steel materials. Especially austenitic steels are extensively researched at BIAS for example of Tetzel et al. (2013). Relating to simulations of materials running through phase transformation it is state of the art to use one single continuous-cooling-transformation-diagram (cct-diagrams) for an entire model consisting of one material. Contrary to this material modelling Berkhout and van Lent (1968) indicated an influence of peak temperature on transformation behavior for S355 steel (St. 52). Fig. 1 shows their result, higher peak temperature leads to longer times for transformation. Thus the peak temperatures affect phase formation behaviour and furthermore the impact of these phases on residual stress formation. Reasonable for different residual stresses are microstructural disparities of the phases. Fig. 2 (a) illustrates phase formation behaviour in view of increasing cooling rate by Loose et al. and fig. 2 (b) depicts the approach of Sakkiettibutra to line out the calculated yield stresses of the different phases to show the reason for appearing residual stresses above yield strength of base materials. According to this the prevailing phase restricts regional maximum of residual stress.

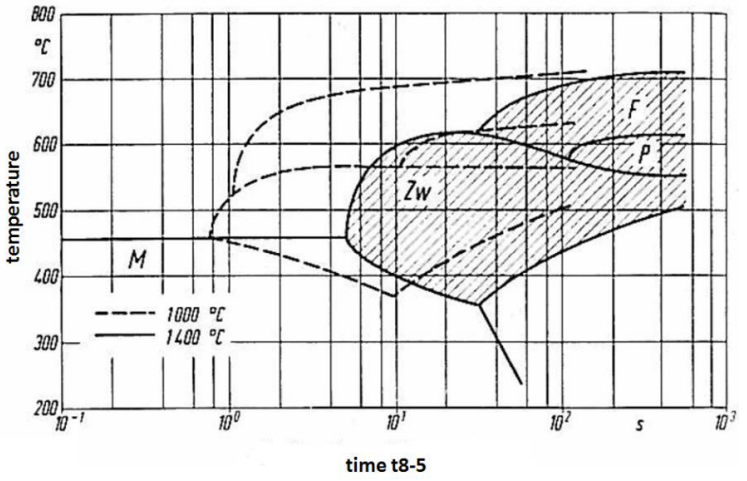

BIAS ID 140993

Fig. 1. Cct-diagrams of S355 for peak temperatures 1000 °C and 1400 °C from Berkhout and van Lent (1968).

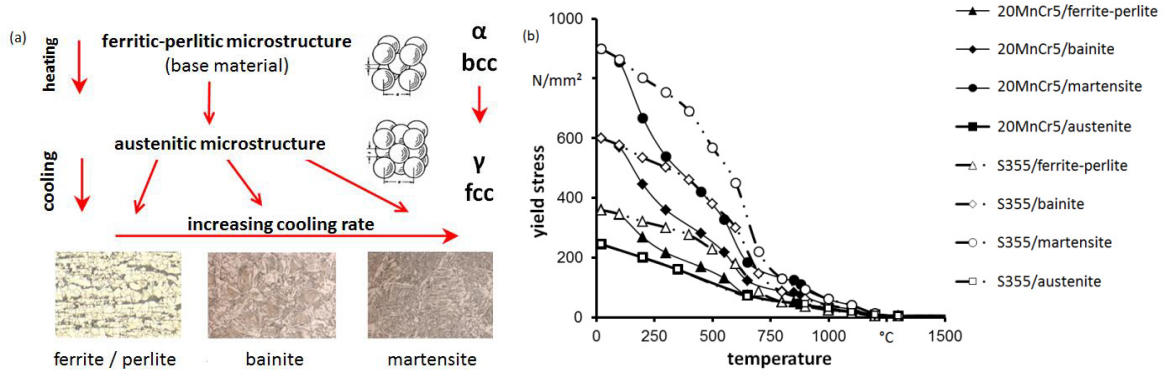

BIAS ID 140994

Fig. 2. (a) Transformation related to cooling rates by Loose et al. (2008) and specific yield stresses of S355 and 20MnCr5 by Sakkiettibutra (2013).

Fig. 3 depicts a simulated temperature profile for thermal forming of S355 steel. Along the width of the heat affected zone (HAZ) a temperature gradient higher than 400 °C is detectable, which causes according to fig. 1 a shift of time for transformation by one power of ten. Compared to measured longitudinal residual stresses the finite element calculation using one cct-diagram leads to a deviant curve and a dissenting maximum peak of this curve, illustrated in fig. 4. Thus the results of the simulation can potentially be more precise.

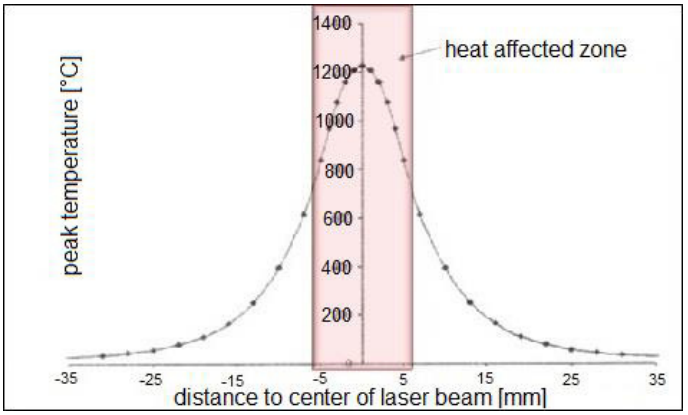

BIAS ID 140995

Fig. 3. Temperature profile of a thermal bending simulation (S355).

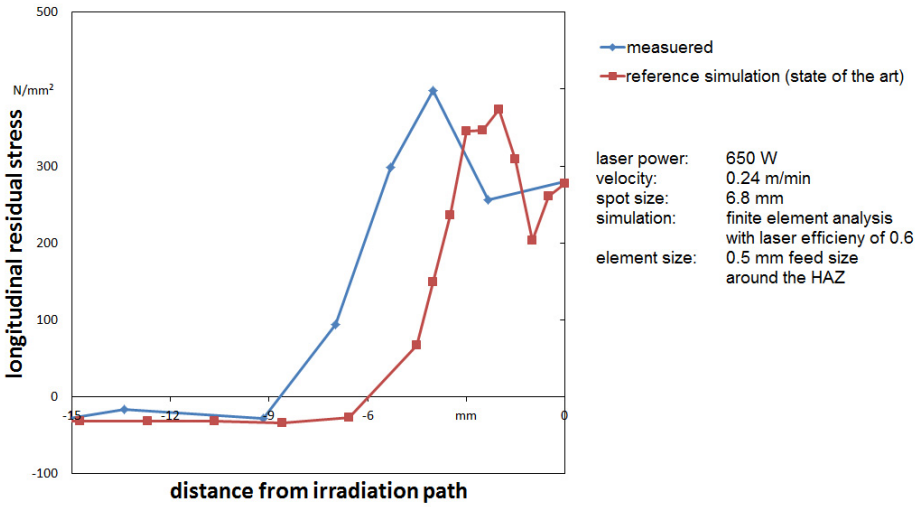

BIAS ID 140996

Fig. 4. Measured longitudinal residual stresses compared to simulation carried out for state of the art modelling.

Residual stresses have got a direct influence on plastic deformation. According to Williams et al. (2008) it is of special interest to know about their development mechanisms and to control residual stresses. This is outlined for knowledge of residual stress formation itself and for its influence on distortions.

Since material modelling may be one of the imprecisions, in this paper the effect of time for transformation because of different austenite grain sizes is outlined by implementing varying cct-diagrams for S355 steel. Peak temperature cycles are transferred to austenite grain sizes. Resulting residual stresses are compared.

2. Simulation setup

2.1. Material modelling

Detecting the general effect of specific transformation behaviors a plate of l = 150 mm length, w = 100 mm width and d = 5 mm thickness is used. The model consists of a finer meshed area around the irradiation path containing 0.5 mm sized elements, highlighted in fig. 5, and a coarser mesh to the edges. The entire model consists of hexagonal elements. Results of the thermal, metallurgical and mechanical calculations are documented at l/2 and the top of the plate, for every node along the width (see fig. 5 measurement line). Numerical calculations are carried out with the software simufact.welding.

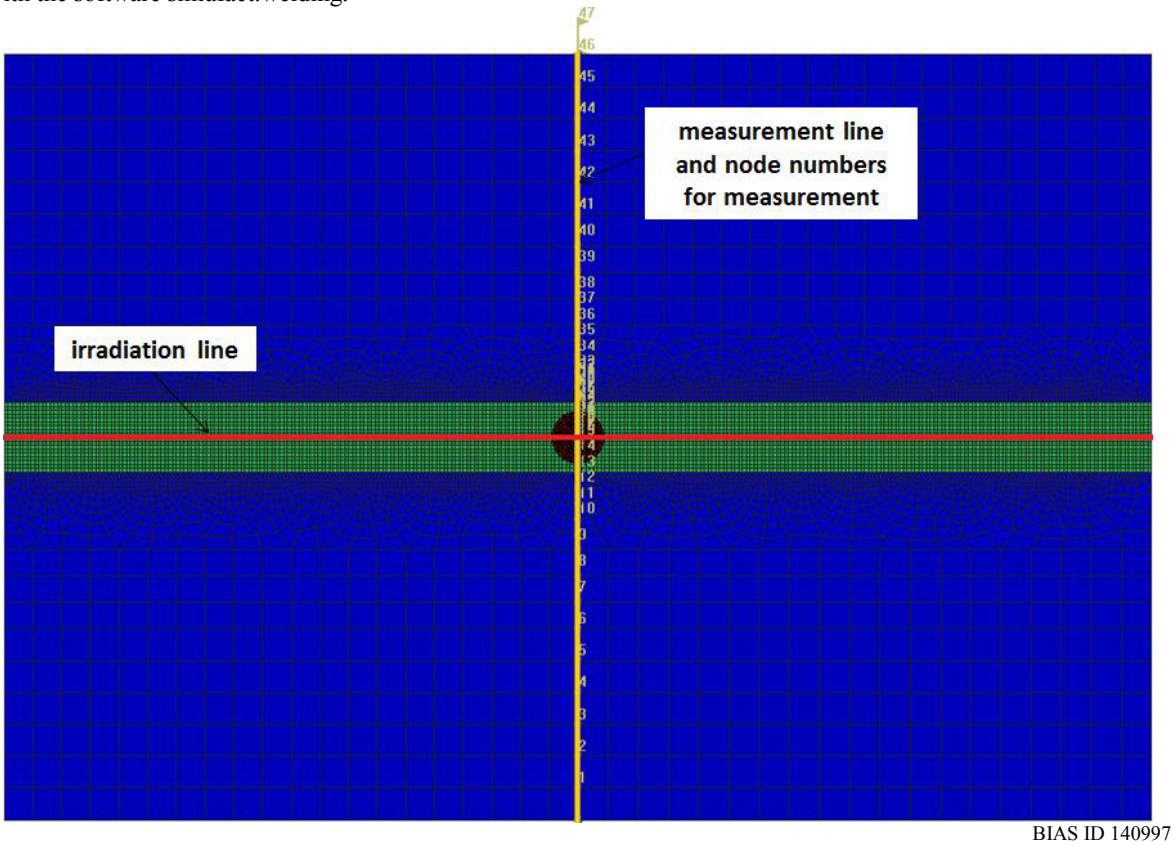

Fig. 5. Meshed model of the plate.

Following the working hypothesis that different austenite grain sizes are leading to varying phase transformation behavior which affects the phase formation and therefore the formation of residual stresses, different cct-diagrams for the material have to be present. Using the JMatPro software those cct-diagrams are calculated with respect to austenite grain size. Focusing on its effect on residual stress formation, different austenite grain size dependent material models for S355 steel are implemented.

In order to point out that the austenite grain size influences transient phase transformation behavior the evolution of austenite grain size related to prevailing peak temperature has to be described. Leblond and Devaux (1984) evolved a model, expressed by equation (1), to calculate austenite grain size D based on the temperature cycle and hence on the peak temperature. Physical constants, $C = 0.4948 \cdot 10^{14}$ mm^4/s and $a = 4$, and $Q/R = 63900$ as activation energy give results pursuant to Sysweld (2014).

$$\frac{d}{dt} D^a = C \cdot \exp(-\frac{Q}{RT}) \quad (1)$$

Based on equation (1) it is possible to line out magnitudes of austenite grain sizes for peak temperatures between AC3 and melting temperature and relevant temperature cycles of the applied process. For different approaches of heating- and cooling-rates per peak temperature, limits related to prevailing temperature-curves are defined. Table 1 contains the austenite grain size ranges used in this paper, calculated for peak temperatures and diverse heating and cooling rates.

Table 1. Calculated austenite grain sizes for appearing temperature cycles.

Peak temperature [°C]	Austenite grain size [µm]	Heating rates [°C/s]	Cooling rates [°C/s]
900	3-5	6800 – 7800	-7000 - -5500
1100	45-65	12000 – 15300	-9000 - -11000
1450	160-210	18500 - 19900	-13900 - -12000

2.2. Material modelling for HAZ approach

For giving a first view on the effect of peak temperatures along the cross-section of the HAZ, a calculation is carried out for three different austenite grain sizes relating to the magnitudes brought out in table 1. For elements affected by temperatures around 1450 °C and 1100 °C the relating material models are implemented. Sizes of the austenite grains are approximated to even numbers, 5 µm for lower temperature (<950 °C), 60 µm for mean temperatures (950 °C-1300 °C) and 200 µm for high temperatures (>1300 °C) are used. Fig. 6 sketches the cross-section of the meshed model and the relation between occurring peak temperature and austenite grain size assumed for the approach. For the high temperature range only two respective midst elements along the irradiation path are used because these are reclusively exposed by the temperature of 1450 °C (fig. 6).

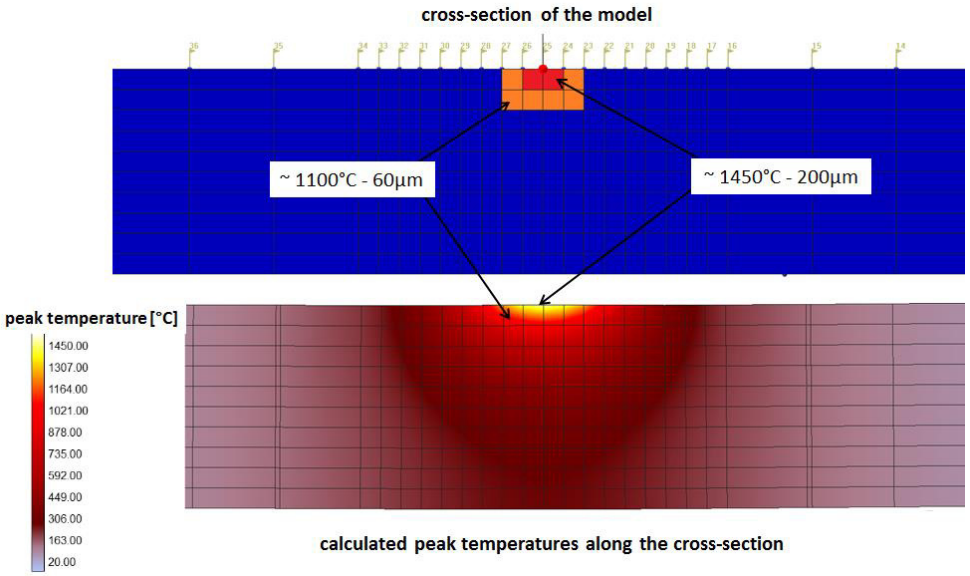

BIAS ID 140998

Fig. 6. Distribution of austenite grain sizes in the HAZ for high temperatures.

3. Experimental setup

As for validation experiments are conducted. Sheet metal made of S355 steel on a special three-point bearing is examined. The three-point bearing is used to ensure a statically determined support and to avoid heat accumulation under the plate. In order to exclude thermal flux ceramic balls are used as bearings. No clamps are used to factor out their influences on material behavior. Fig. 7 shows the setup including thermal measurement. For thermal measurement thermal elements type k, a thermo camera by Infratec and a two-colored pyrometer Impac IGAR 12 LO are used because every of these techniques is precise for a specific range of temperature. The specimen holder is displayed in the enlarged section in the bottom left corner of fig. 7. The experiments have been conducted via disk laser TruDisk 8002 by Trumpf. The laser parameters are kept constant during all of the simulations and experiments. Laser parameters are listed in Table 2.

Table 2. Laser parameters for simulation.

laser power [W]	velocity [m/min]	spot size [mm]
650	0.24	6.8

Residual stresses have been measured by Stresstech GmbH using X-ray diffractometry along the width of the plates.

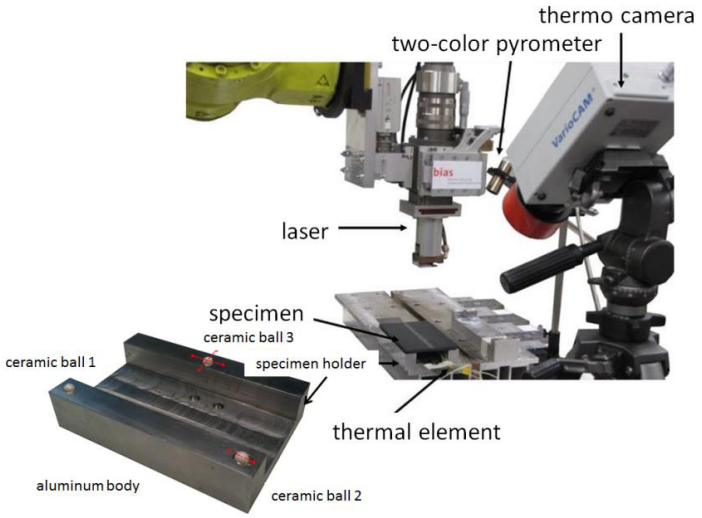

BIAS ID 140999

Fig. 7. Experimental setup like described by Sakkiettibutra (2013).

4. Results

4.1. Fundamental effect of austenite grain sizes on transformation on residual stress

Getting a general idea of the impact of austenite grain sizes ten different ones between 3 microns and 800 microns have been chosen. The used austenite grain sizes are listed in Table 3.

Table 3. Austenite grain sizes for material setup.

Austenite grain size [µm]									
3	5	7	10	30	60	100	200	400	800

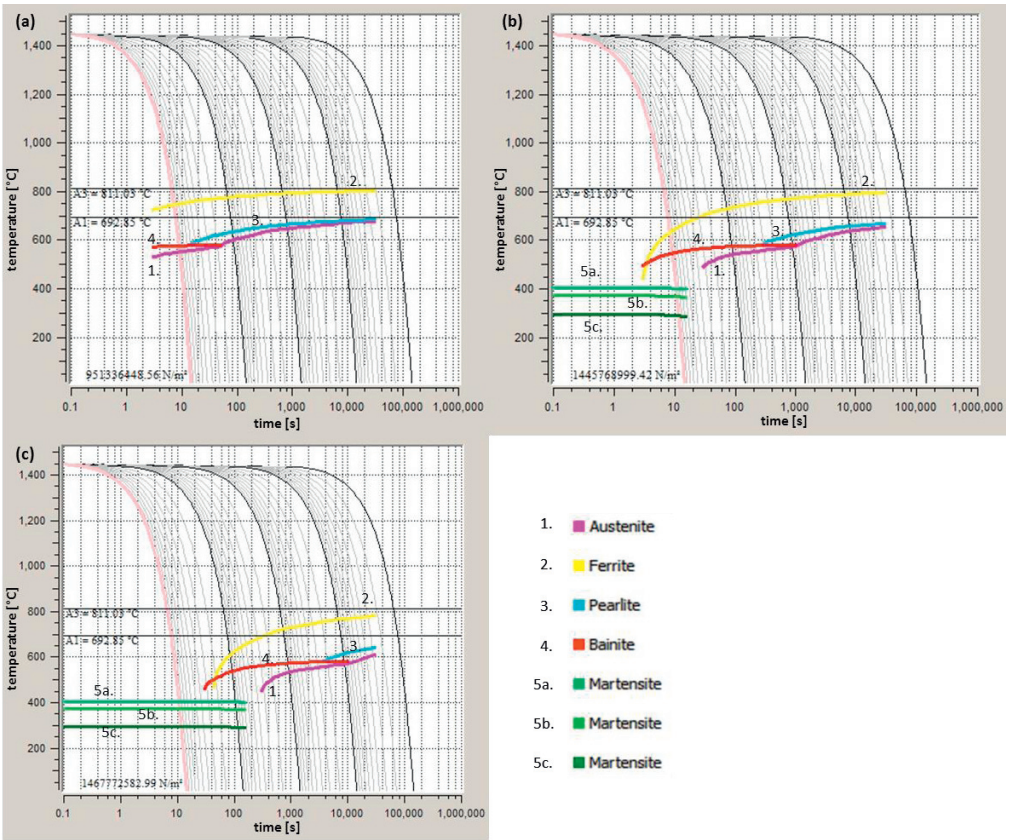

BIAS ID 141000

Fig. 8. Cct-diagrams for S355steel and 3 µm (a), 60 µm (b) and 800 µm (c) from JMatPro.

Fig. 8 depicts three different cct-diagrams for 3 microns (a), 60 microns (b) and 800 microns (c) austenite grain size. The relation described in chapter 1, larger austenite grains lead to longer times for transformation, is confirmable for the material modelling. Ferrite-formation for example is beginning around 3 s for 60 µm (fig. 8 (b)) and around 40 s for 200 µm (fig. 8 (c)) austenite grain size. The calculations result in diversifying distributions of residual stresses. The most conspicuous attributes are the different magnitudes of these distributions, varying between s2 = 248 MPa and s1 = 550 MPa and the widths of the residual stress plateau between w1 = 13.1 mm and w2 = 36.3 mm. Fig. 9 exemplarily shows simulation results, the formations of residual stresses in longitudinal direction, for each node along the cross section at the top of the plate for three different austenite grain sizes. Smallest austenite grain size chosen leads to highest residual stress peak, increasing austenite grain sizes result in a residual stress peak lower than this one. Fig. 10 depicts the impact of austenite grain size on residual stresses, the maximum value is calculated for the smallest austenite grain size but the minimum is shown for a mean grain size of 100 µm. For higher austenite grain sizes the residual stress level increases again. Also illustrated in fig. 10 the width of the residual stress plateau is indicated as increasing for increasing austenite grain sizes up to 200 µm, then it stops spreading. Preliminary studies point out that elements featuring 0.5 mm feed size are small enough to picture out the gradients of 1.4301 steel for thermal forming simulation. Fig 9 is giving a first view on the possibly imprecise representation of residual stress profiles for 0.5 mm feed size and materials with phase transformations. The profiles minima aren't calculated accurately for every grain size, seen for 30 µm in fig. 9. Smaller element sizes around the HAZ can give a view on the results for a more precise modelling.

Contrary to the known and measured M-profiles in the work of Sakkiettibutra et al. (2011) (seen in fig. 4) inherent compressive stress is calculated for some of the austenite grain sizes. Therefore the interactive effects of different austenite grain sizes on each other have to be observed because the heat flow and the temperature are varying compared to the state-of-the-art calculation.

The influence of austenite grain size on magnitudes of residual stress formation could have been shown. For further investigations the sensitivity of the model has to be investigated. For smaller austenite grain sizes the residual stresses seem to dissipate faster by distance from irradiation, possibly the larger number of grain surfaces cause a better transfer of distortions and therefore residual stresses.

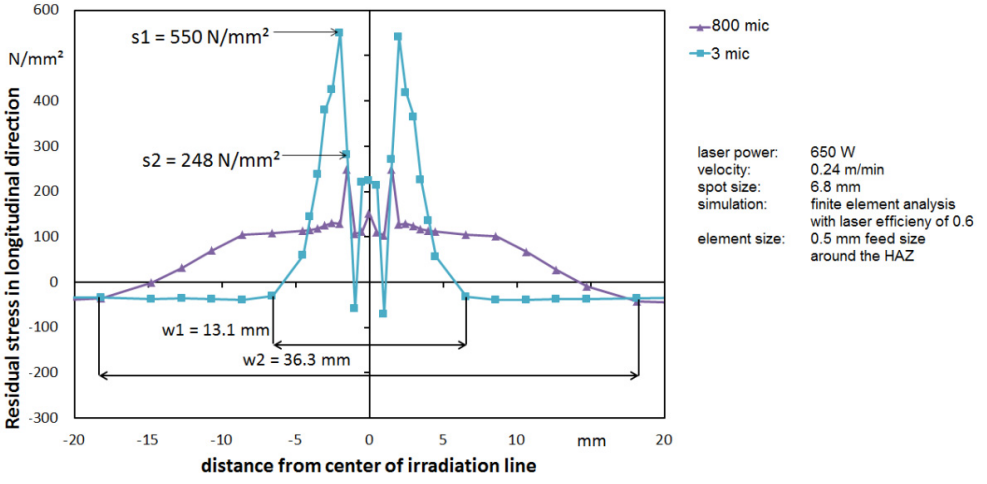

BIAS ID 141001

Fig. 9. Longitudinal residual stress formation relating to austenite grain size in microns.

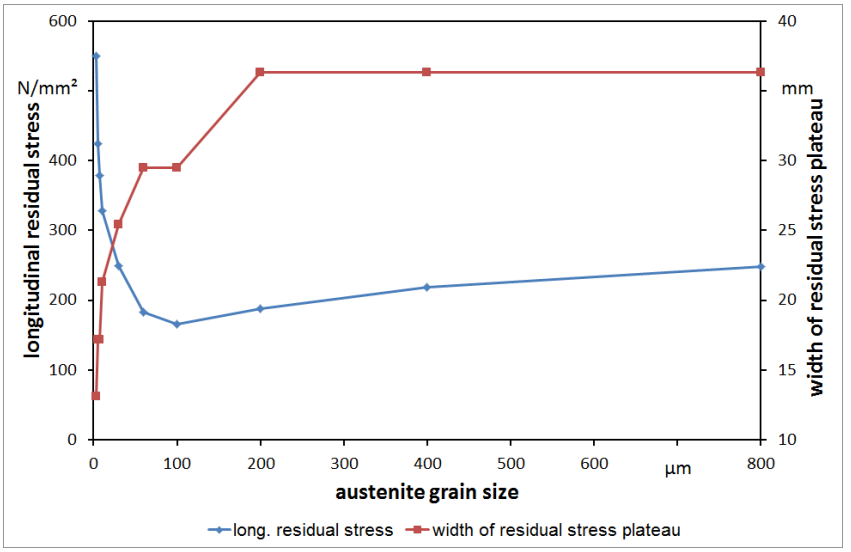

BIAS ID 141002

Fig. 10. Size effect of austenite grain size on maximum residual stress and width of residual stress plateau.

4.2. Approach for peak temperatures in the heat affective zone

The simulation with three different cct-diagrams leads to a peak of longitudinal residual stresses at the same stress-level like it is measured in the experiments. Compared to the reference calculation using state of the art material property for S355 steel this modelling technique improves the magnitude but not the distribution along the width.

Especially for continuative simulations of fatigue strength tensile residual stresses are of special interest because these stresses are the failure criterion. Thus a more accurate calculation in the thermal simulation improves the accuracy of further investigations. Results of reference calculation and the separated material modelling compared to measured residual stresses are shown in fig. 11. The maximum peak value of residual stress is more precisely calculated (left oval in fig. 11). Instead of that the curve progression is formed more imprecise because an additional peak in the midst of the plate is developing (right oval in fig. 11) dissenting to measured results.

Thus accuracy of the model according to the number of selected austenite grain sizes has to be examined since the results aren't conclusive and more precise austenite grain size partitions can be of use. The influences of the different material properties in the model on each other have to be lined out as well due to the described variation of heat flow and temperature during simulation.

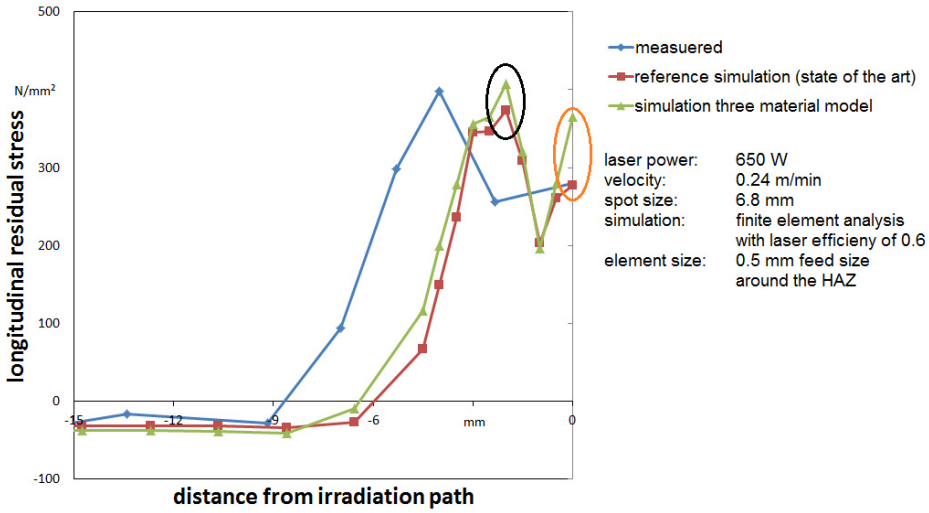

BIAS ID 141003

Fig. 11. Comparison of measured longitudinal residual stresses and simulation results, reference S355 and local implemented material properties.

5. Conclusion

A numerical modelled implementation of austenite grain sizes into material properties is presented. The effect of austenite grain size on the formation of residual stresses can be shown exemplarily for longitudinal residual stresses. A first implementation of more than one cct-diagram brings out that local material modelling can increase accuracy for maximum residual stress peak of simulation but not for curve progression whether these results have to be confirmed relating to material model interaction.

Acknowledgements

We would like to thank the German Research Foundation (DFG) for funding the project "Spitzentemperaturabhängige Eigenspannungsausbildung umwandelnder Stähle" from which the results released in

this paper origin. We also would like to thank Simufact Engineering GmbH, especially Dr.- Ing. Sakkiettibutra for providing the material data from JMatPro.

References

Jeswiet, J., Geiger, M., Engel, U., Kleiner, M., Schikorra, M., Duflou, J., Neugebauer, R., Bariani, P., Bruschi, S., 2008. Metal forming progress since 2000. CIRP Journal of Manufacturing Technologies 1:2–17

Neugebauer R., Scheffler S., Poprawe R., Weisheit A., 2009. Local laser heat treatment of high strength steels to improve formability, (WGP). Production Engineering Research and Development 3, 347–351

Vollertsen, F. 1996., Laserstrahlumformen – Lasergestützte Formgebung: Verfahren, Mechanismen, Modellierung. Meisenbach, Bamberg. (in German)

Vollertsen, F., 1993, An analytical model for laser bending. Laser in Engineering, Vol. 2, 261-276

Tetzel, H., Grden, M., Vollertsen, F., 2013. Stress analysis based on strain measurement in sheet metal laser bending. Production Engineering Research and Development 7, 647-655

Berkhout, C., van Lent, P., 1968. Anwendung von Spitzentemperatur-Abkühlzeit (STAZ)-Schaubildern beim Schweißen hochfester Stähle. Schweißen und Schneiden 6, 256-260. (In German)

Loose, T., Sakkiettibutra, J., 2008. Leistungsmerkmale der Schweiß-Struktursimulation. Schweißen und Schneiden 9, 487-491 (in German)

Sakkiettibutra, J., 2013. Modellierung thermisch bedingter Formänderungen und Eigenspannungen von Stählen zum Aufbau von geregelten Prozessen. Strahltechnik vol. 51, BIAS-Verlag. Bremen (in German)

Leblond, J. B., Devaux, J., 1984. A new kinetic model for anisothermal metallurgical transformations in steel including effect of austenite grain size. Acta Metallurgica Vol. 32 No.1, 137-146.

Williams, S., Morgan, S., Wescott, A., Poad, M., Wen, S., 2008. Stress engineering-Control of residual stresses and distortion in welding. International Workshop on Thermal Forming and Welding Distortion (IWOTE'08). Eds.: Vollertsen, F., Sakkietibutra, J., Strahltechnik vol.31, BIAS-Verlag, Bremen, 229-239

Sakkiettibutra, J.; Vollertsen, F., 2011. Differences in the residual stress development between laser-formed austenitic and mild steel sheets. In Proc. Thermal Forming and Welding Distortion (IWOTE'11). Ed. Vollertsen, F. BIAS-Verlag, Bremen, 145-167

Sysweld Manual, 2014. Calculation of grain size, 136-137